

Operating Limits and Control Variables in Photovoltaic Solar Plants with a Net Effective Capacity of 5 MW Connected to the SIN in Colombia



Cristian Rosas^{ID}, Julieth Avendaño^{ID}, Cesar Hernández*^{ID}

Facultad Tecnológica, Universidad Distrital Francisco José de Caldas, Bogotá 111931, Colombia

Corresponding Author Email: cahernandezs@udistrital.edu.co

Copyright: ©2024 The authors. This article is published by IIETA and is licensed under the CC BY 4.0 license (<http://creativecommons.org/licenses/by/4.0/>).

<https://doi.org/10.18280/ijepm.090308>

Received: 29 February 2024

Revised: 19 March 2024

Accepted: 16 July 2024

Available online: 26 September 2024

Keywords:

solar plants, SIN, STN control, SCCR, HVRT, LVRT

ABSTRACT

This document delineates the central supervision and control variables for photovoltaic parks that possess a net adequate capacity or power exceeding 5 MW, which are interconnected to the National Interconnected System (SIN) serving as a backup to Colombia's Regional Transmission System (STR). To establish a comprehensive understanding of the operating limits and control variables for photovoltaic solar plants with a net adequate capacity or maximum power of at least 5 MW, a research and analysis methodology was developed in accordance with the regulatory framework in Colombia. This methodology aims to underpin the regulatory parameters and operational guidelines for enhancing the efficiency and compliance of these energy systems.

1. INTRODUCTION

Renewable energies and energy efficiency have become the most critical issues given the transition to implementing new technologies that are more sustainable and reliable in their integration into the interconnected electricity system. The ones that have stood out the most in recent years are photovoltaic and wind generation, as well as their usefulness in controlling the different electrical variables within the connection point to the electricity system.

The strength of photovoltaic systems has manifested itself in all corners of the world, but Asia has been the most dynamic continent. The photovoltaic sector has added 76 GW to its generation fleet, one gigawatt more than in 2020. China has been the world's leading photovoltaic (PV) power for another year, with 53 GW of new capacity. India installed 10.3 GW, Japan installed 4.4 GW, and South Korea installed almost 3.6 GW. The following three nations in the ranking are the United States of America with 19.6 GW of new PV capacity, Brazil with 5.2 GW and Germany with 4.7 GW. Additionally, the Netherlands and Spain installed more than 3 GW; these figures show that wind and photovoltaic energies together add up to 88% of the new renewable capacity installed in 2021 [1].

Meanwhile, in the case of Colombia, the available sources of solar resource information indicate that the country has an average irradiance of 4.5 kWh/m²/d, which exceeds the world average of 3.9 kWh/m²/d; particular regions of the country, such as La Guajira, a good part of the Atlantic Coast and other specific regions in the departments of Arauca, Casanare, Vichada, and Meta, among others, have radiation levels above the national average that can reach the order of 6.0 kWh/m²/d, a resource comparable to some of the regions with the best

resources in the world, such as the Atacama Desert in Chile or the states of Arizona and New Mexico in the United States. According to estimates made in Colombia, there are around 9 MWp of installed solar photovoltaic capacity, corresponding to private systems, professional applications, and solutions in non-interconnected areas (it is assumed that, for the most part, they are made up of low-capacity systems, less than the order of 10 kWp). In addition, in recent years, there has been information on the installation of a good number of systems with capacities greater than ten kWp (some in the order of several hundred kWp) both in the Non-Interconnected Zones (ZNI) and in the commercial and industrial sectors [2]. Currently, through the UPME's new Information and Knowledge Management System in FNCER, the necessary management is being carried out to encourage this type of project through its voluntary registration by developers, installers, and users interested in sharing such information with the general public [3]. A simplified diagram of this system is shown in Figure 1.

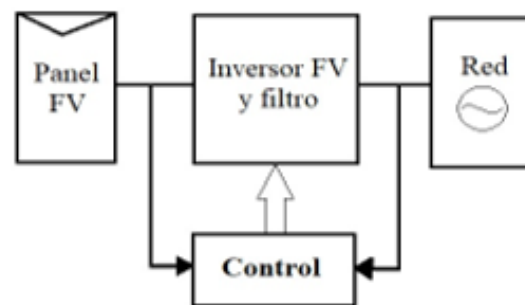


Figure 1. Grid-connected photovoltaic system

Based on the technical characteristics of photovoltaic systems, they must meet certain operating features and requirements in the control of electrical variables that may occur at the point of connection to the grid, providing reliability to the system.

This article gives an initial guideline so that the new photovoltaic systems that want to be integrated into the national interconnected system comply with the regulatory requirements as backup systems in Colombia from 2025, it will be mandatory for these parks to help maintain the stability of the electrical system, summarizing the above, solar parks must be part of the support for the different electrical disturbances that may occur, increasing reliability and not only being participants as generation units but also helping to maintain, above all, the frequency ranges and tension.

It should be noted that in Colombia, no photovoltaic solar parks comply 100% with the required regulatory requirements. Based on this article, the Colombian regulatory framework, and the particular conditions of solar park generation and installation, one can begin to implement the control systems practically so that they, in turn, function as backup systems.

Advantages:

- There is insufficient information on photovoltaic solar parks that function as backup systems in Colombia.
- Within the sociopolitical context of Colombia, forced displacement has generated exponentially increasing cities' population in recent decades, generating an overload in the electrical system. This article proposes control systems for the different photovoltaic solar parks that can help mitigate these types of disturbances in the system.
- In some regions of Colombia, the distribution systems are radial type. Therefore, it is isolated because they do not have an appropriate return as in a ring-type system when a failure occurs in a node of the system. This occurs especially in the Caribbean region, where most photovoltaic solar parks are intended to be built. This would allow said parks to function as a local backup system.

For countries with the same distribution system problems, this variable control under the Colombian regulatory framework can be a starting point, thus encouraging this type of renewable generation.

2. TECHNICAL SPECIFICATIONS OF CONTROL VARIABLES

This chapter will describe the control and supervision variables applicable to photovoltaic solar plants with respect to the connection point to the SIN in accordance with Colombian regulations and guidelines. Photovoltaic solar plants must receive and manage local and/or remote setpoints of the following variables: active power, reactive power, frequency, and voltage. For this, the different modes of supervision and/or control must be considered, which are:

- Open Loop [LA]: In an open loop system, no feedback is used to adjust or correct the system based on its current performance. Instead, control commands are issued based on assumptions or estimates about how the system should behave. It is used to test equipment communications and for maintenance work. It also serves to have control in local mode in case of communications failure with the network operator.

- Closed-loop [LC]: A control system in which feedback adjusts and maintains a variable or process within specific parameters or desired values. This allows control to be carried

out remotely from a SCADA at a higher level in the network operator's facilities.

- Control about statism: It is the control related to the percentage.

- Variation of a variable concerning the variable that will carry out the percentage control of it, which must be limited to operating limits.

Next, a description of each type of control that can be presented according to the variable to be controlled will be made, relating block diagrams and graphs corresponding to the kind of control [4].

3. ACTIVE POWER

This variable must control between 10% and 100% of the nominal power the photovoltaic generating plant declares at the connection point. So, in all modes of operation, you need to be able to control power in these ranges. A relationship that can explain this condition in detail is described in Eq. (1).

$$0.1 * P_n \geq P_{PC} \geq 1 * P_n \quad (1)$$

where P_{PC} is the power supplied at the connection point and the nominal power declared by the photovoltaic park.

According to the above provisions of article No. 15 of CREG 060, the maximum adjustment range that the control ramp must have been determined, which is 14% of the declared nominal power, see Figure 2.

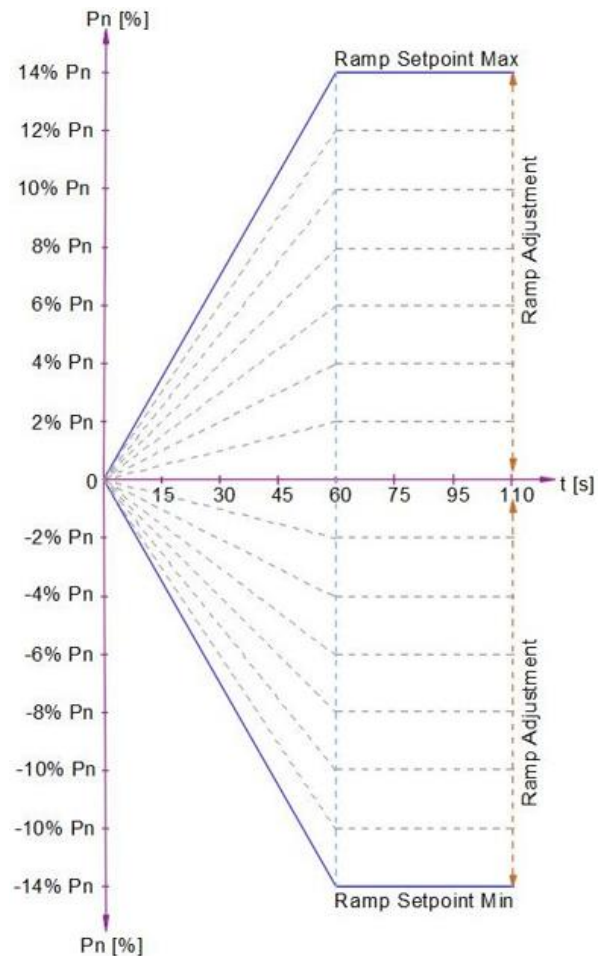


Figure 2. Graph of ramp control according to the limits established in the Creg 060

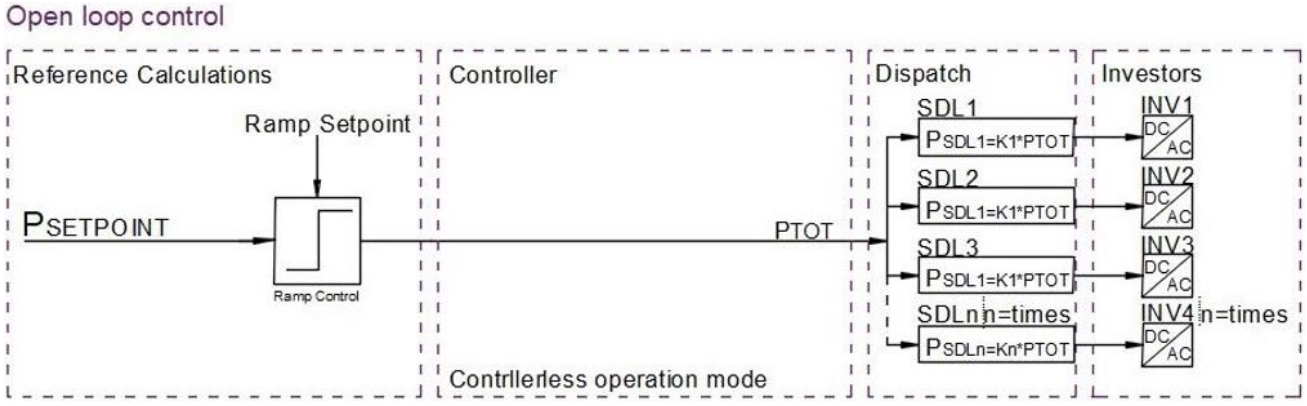


Figure 3. Block diagram active power control mode in open loop

In Figure 2, we can see that the adjustment can be negative or positive, reaching and positive, to reach objective values both above and below the value provided at the time of the disturbance according to the requirements of each control mode.

It is also evident that the active power slope the operator assigns allows the system to reach the desired target value quickly or slowly [5].

Two scenarios are established for power control: one in Open Loop (OL) and one in Closed Loop (CL).

3.1 Open loop active power control

The open loop active power control mode considers a power value (PCONSIGNA) which is the ultimate goal of the control and can be managed by the grid operator and the solar park operator. Figure 3 illustrates the simple control in this mode of operation.

In this mode of operation, the PCONSIGNA will be the target active power, which will pass through the ramp control, and vary its behavior based on the ramp setpoint. For this, the ranges of variation are between 0.1% and 14%. The latter percentage will be the maximum ramp value that can be assigned. This ramp control will take the necessary steps to reach the desired target value by giving the PTOT output as the output; this variable will be the total active power ratio we want at the connection point.

It is essential to know that each solar park is represented by a set of "Smart data loggers" [6] which allows a record and monitoring of each stage of solar panels, this equipment must be assigned a value of "K" that will be a constant percentage that each set of panels can supply according to its installed capacity. The K value varies depending on weather conditions, possible damage to the panels, and the number of independent generation modules, among other things. "K" is a percentage of the power setpoint distributed over the number of available devices. In the block diagram PSDL represents a different group of "Smart data loggers", described in Eq. (2).

$$P_{TOT} = P_{SDL1} + P_{SDL2} + P_{SDL3} + \dots + P_{SDLn} \quad (2)$$

Knowing that each PSDL is the same as what is expressed in Eq. (3).

$$\begin{aligned} P_{SDL1} &= K_1 * P_{TOT}; P_{SDL2} = K_2 * P_{TOT}; \\ P_{SDL3} &= K_3 * P_{TOT}; P_{SDLn} = K_n * P_{TOT} \end{aligned} \quad (3)$$

If the sum of each PSDL must be equal to PTOT, we can

conclude that the sum of all "K" must be equal to "1" if values per unit are considered, this could be represented as shown in Eq. (4).

$$K_{TOTAL} = K_1 + K_2 + K_3 + \dots + K_n = 1pu \quad (4)$$

In the output of the PSDL, the inverters associated with each set of panels of the photovoltaic park are represented. These are the ones that in the end will carry out the power directive as requested, as well as the existing capacity in each set.

3.2 Closed-loop active power control

Most of the considerations described in open-loop control mode are considered in closed-loop active power control which maintains the ramp control parameter with its respective setpoint settings.

In the output of this ramp controller, there will be a variable called PSP (Power Setpoint) of closed-loop PI, having as a feedback variable the one registered at the connection point, called PPC. From the recorded difference, a gain factor will present a variation concerning an integration time, including or decreasing the power needed so that the PCONSIGNA values are as close as possible to the power recorded at the connection point [7].

PSP is the output of the setpoint change ramp, which is also the input of the PI setpoint. The ramp is a parameter entered from the SCADA or IHM that ranges from 0.1-0.14. Power per unit is not left in physical values since this ramp can vary depending on the generation characteristics of the photovoltaic solar park. In the PI value, the power grid operators tell us how fast or slow the response of the photovoltaic park is required.

Each control mode incorporates a ramp algorithm, which adjusts from an old setpoint to a new one at a speed that can vary between 0.1% and 14% of the declared nominal power per minute. This mechanism complies with Colombian regulations, ensuring smooth transitions to prevent adverse impacts on other electrical variables and to keep correction times within acceptable limits.

In all control modes, devices known as Smart Data Loggers (SDL) are used, whose technology varies according to the manufacturer. These devices monitor and communicate with the available inverters, assigning the setpoint equitably among them. The significance of the SDL lies in their ability to manage the operation of electrical equipment in the generation of energy at the solar park, depending on their availability. This article addresses how to adjust each electrical variable according to the requirements, until reaching a determined

target setpoint value, to which the SDL must adjust. Since the description and operation of these devices vary according to the manufacturer, as well as their communication architecture, they do not adhere to a uniform standard and depend on the configuration and capacity of each generation unit.

Considering the approach for this control mode, a block diagram is designed, as described in Figure 4.

Figure 4 shows what is described by Eq. (5).

$$Error = P_{SP} - P_{PC} \quad (5)$$

Closed loop control

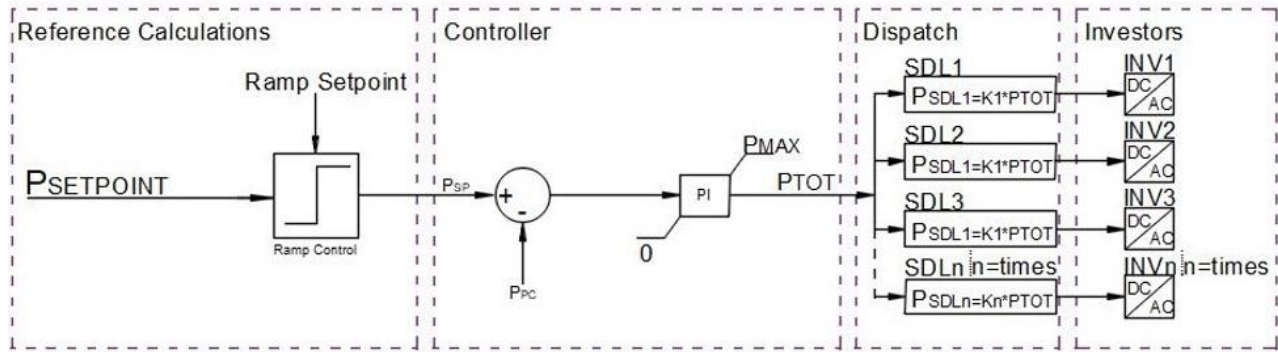


Figure 4. Block diagram of closed-loop active power control mode

3.3 Frequency control based on active power

Frequency control based on active power must consider new feedback that will depend on frequency variations at the connection point and the maximum capacity that plants can supply based on their declared ability [8].

Considering the definition of frequency statism in Annex 1 of the CNO1531, which determines the procedure for determining the characteristics of the active power/frequency control of photovoltaic solar plants, frequency statism defines the power variation for each unit of percentage frequency variation and is expressed in Eq. (6).

$$Re = \frac{\Delta f / f_{nom}}{\Delta P / P_{nom}} \times 100\% \quad (6)$$

where,

Δf : Magnitude of frequency variation in Hz applied.

Δf : $f_{final} - f_{initial}$.

In this case, a PI is contemplated, assigning the necessary power so that the energy reaching the connection point is as close as possible to the initial target value. That said, the most important variables of this control mode are:

Gain (P): This will be a minimum power we want to keep within a permissible margin of error.

Integral Time (I): This is the time it takes for each assigned power gain scale to start a new scale.

The goal of the PI is to reach the desired value, in this case the margin of error with a gain and integration time that the operator assigns.

f_{nom} : Nominal frequency of the system Hz.

ΔP : Magnitude of power variation due to frequency variation.

ΔP : $P_{final} - P_{initial}$.

P_{nom} : Nominal power of the park.

According to Eq. (6), the following initial parameters must be taken into account:

Dead Band: $\pm 120\text{mHz}$.

Statism: $R_f(2\% - 6\%)$ Must be assigned from the start.

$P_{initial}$: Varies according to what is available in the park at the time of the disturbance.

F_{final} : The overfrequency that occurs in the disturbance at the coupling point.

Sub-frequency: $f_{nom} - B_{muerta}$.

Oversfrequency: $f_{nom} + B_{muerta}$.

Once these parameters have been defined, it will be possible to control the frequency concerning the statism ranges established in the standard, and the operating ranges of the frequency normal at the coupling point. Table 1 shows the characteristics of these operating ranges.

Table 1. Frequency ranges for control

Frequency (Hz)	Rank	Control
<57.5		In this case, you must have an under-frequency protection system to protect the photovoltaic park.
57.5 59.0	Sub-frequency	If the PV park can provide more power than is required during the disturbance, it must assign a new setpoint.
<59.88 ($f_{nom} - B_{muerta}$) 59.88 ($f_{nom} - B_{muerta}$) 60.0	Frequency of operation	The control system does not operate in this frequency range, the park must operate normally.
60.12 ($f_{nom} + B_{muerta}$) >60.12 ($f_{nom} + B_{muerta}$) 61.5 63.0	Overfrequency	If the wind farm is above 10% of the declared rated power at the time of disturbance, it must assign a new setpoint value. The supplied power must be brought to 0, so a protection system must decouple the park at the connection point.
>63.0		

In Colombia, the frequency, voltage and Pn/Q ranges in Table 1 are based on CREG resolution 229 of 2021, and on the IEEE Standard for Interconnection and Interoperability of Distributed Energy Resources with Associated Electric Power Systems Interfaces. With the data in Table 1, the behavior graph of the photovoltaic plant for this control mode is obtained; considering the statism ranges described in the standard, the frequency control graph corresponds to Figure 5.

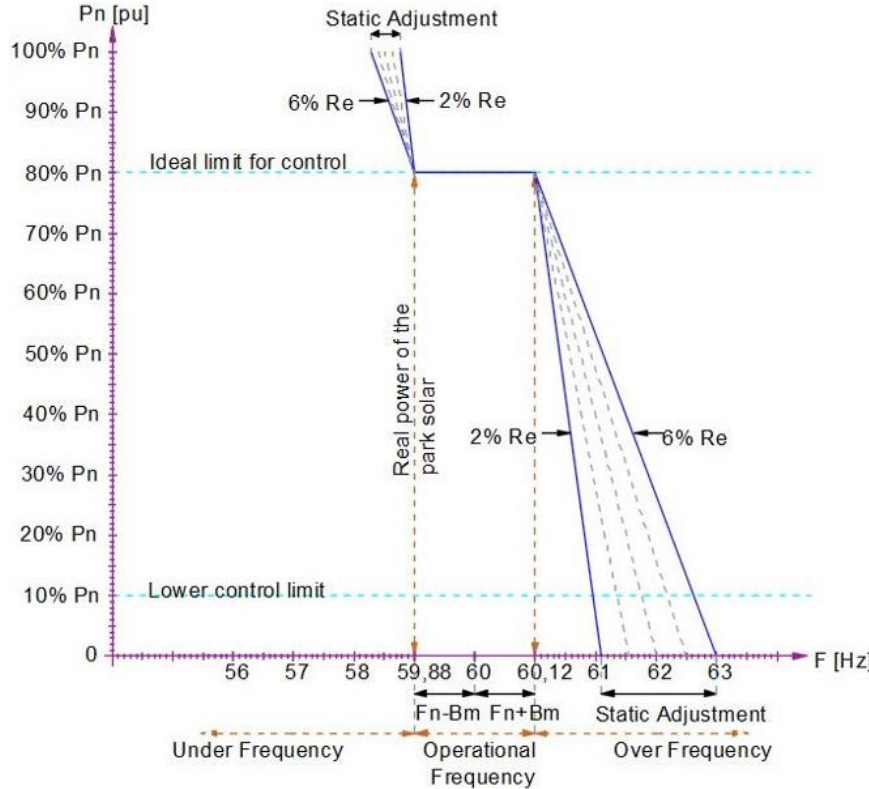


Figure 5. Frequency control graph according to statism setting

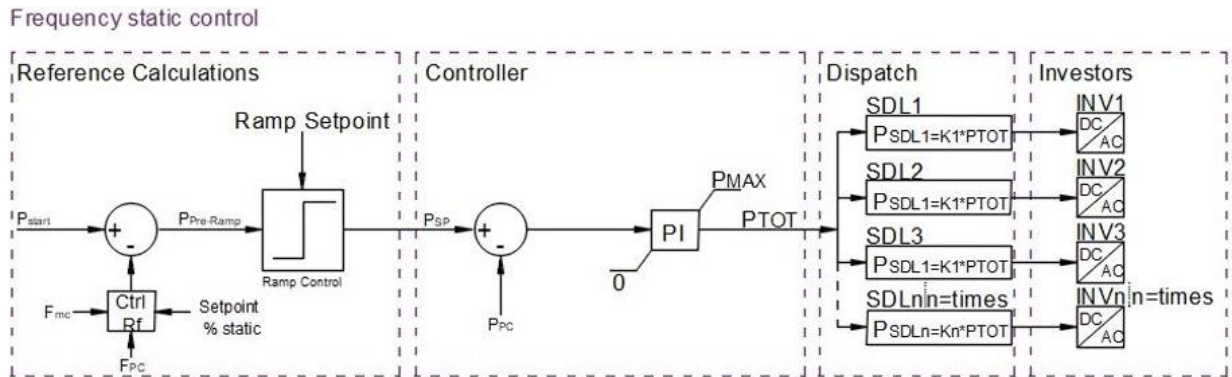


Figure 6. Block diagram frequency control mode

The considerations described for closed-loop active power control are maintained in this control mode. Still, new feedback is contemplated that will depend on the existing frequency at the connection point (and may be adjusted based on the percentage of statism assigned by the operator, taking into account the ranges established in the standard F_{PC}).

To carry out the frequency control, the changes in the active power supplied at the connection point are taken into account, for this Eq. (6) is used, where it will be cleared leaving a new equation represented by Eq. (7).

In Figure 5, it can be seen that the slope of the ramp varies according to the statism slogan. Therefore, the higher the statism value, the lower the slope of the ramp, which allows a greater range of frequency control, but its response time will be slower, the higher the slope of the ramp control the faster the response time will be.

With the above in mind, the block diagram described in Figure 6 is designed.

$$P_{final} = P_{initial} \pm \frac{(f_{final} - f_{initial}) * P_{nom}}{Rf * f_{nom}} \quad (7)$$

where,

P_{final} : New nominal power value to be reached.

$P_{initial}$: The power at which the photovoltaic park is at before the frequency disturbance.

f_{final} : Nominal power of the declared photovoltaic park.

$f_{initial}$: Disturbance that you want to correct.

$f_{initial}$: Frequency before the disturbance the system was

working on.

f_{nom} : Nominal system frequency in Hz.

R_f : Percentage of stasis assigned in frequency control.

The behavior of the frequency control will depend on the frequency range in which it is located. If the disturbance is due to over frequency, the ramp should descend, and if it is due to sub frequency, the ramp should ascend, as shown in Figure 5.

Eq. (7) is determined by solving the P_{final} of Eq. (6), the values that were assigned to replace in the equation, which is a case that can occur in the photovoltaic solar park. Considering that the control will only act up to the maximum operating ranges of plants, established in the standard if these ranges are exceeded, the park's protection systems must act to safeguard the equipment that comprises it. Likewise, a minimum change power must be established, which will depend on the stasis adjustment; the above guarantees that the park can perform frequency control with the real power it has in the photovoltaic park.

To explain this control mode, a static value was assigned, which specifies the different limits and behaviors according to their percentage. The initial power that will be available in the park during the disturbance varies. Between 0.0 to 1 value per unit (pu), an initial frequency that will be the one that requires correction and a change or final frequency that varies 0.1 Hz concerning the initial frequency, it is essential to highlight that the smaller the difference, the smaller the margin of error, therefore by decreasing this frequency delta the margin of error in the control mode correction will be. From this assumption, the formula helps us determine the amount of active power required for every 0.1 Hz to be corrected. This means that a new absolute value must be determined if 1 Hz needs to be corrected at the connection point. By the following division, "1Hz/0.1Hz," the result will be "10". By multiplying this absolute value with the result of Eq. (7), it will be known how much active power must be supplied to reach the desired frequency value. This case will only work in a percentage of stasis that will be previously assigned, showing that the higher the percentage of stasis, the faster the response will be.

Considering that the control will only act up to the maximum operating ranges of the photovoltaic plants established in the standard, if these ranges are exceeded, the protection systems of the park must act to safeguard the equipment that composes it.

In the same way, a minimum change power must be established which will depend on the stasis adjustment, the above is to guarantee that the park can perform frequency control with the real power counted in the photovoltaic park. To explain this minimum power of change in detail, the following example is given:

Assuming a percentage of stasis and two frequency behaviors, one initial and one final, with a difference between them of 0.1 Hz, it is important to note that the smaller the difference, the smaller the margin of error. In order to determine the frequency input for each 0.1 Hz change delta, we will assign values in Eq. (7) assuming that:

P_{final} : This value is calculated from (8) and it will be given in per unit values [pu].

$P_{inicial}$: For this example, 0.8 pu will be taken.

$P_{inicial}$: Declared nominal power of the photovoltaic park 1 pu.

f_{final} : Disturbance frequency at overfrequency and 60.13Hz will be taken.

$f_{inicial}$: Frequency limit before disturbance and shall be 60.12 Hz.

f_{nom} : Nominal Frequency 60Hz.

R_f : 6% statism rate, see Eq. (8).

$$P_{final} = 0.8 \text{ pu} - \frac{(60.22 \text{ Hz} - 60.12 \text{ Hz}) * 1 \text{ pu}}{6\% * 60 \text{ Hz}} = 0.772222 \quad (8)$$

To know the change in power per unit, the difference concerning the initial power is determined, which is represented by Eq. (9).

$$\begin{aligned} P_{minima de cambio} &= P_{inicial} - P_{final} \\ &= 0.8 \text{ pu} - 0.7722 \text{ pu} = 0.027778 \text{ pu} \end{aligned} \quad (9)$$

This indicates that it must stop supplying for every 0.1 Hz of change with a statism of 6%. It is used to calculate the maximum active power control capacity based on the park's actual capacity.

Therefore, it is possible to determine the number of steps that must be taken from the initial power in which the park is located about the minimum capacity of the controller. For the previous case, a new variable is assigned, see Eq. (10).

$$K_p = \frac{P_{inicial}}{P_{minima de cambio}} = \frac{0.8 \text{ pu}}{0.027778 \text{ pu}} = 28.8 \quad (10)$$

In this way, it is possible to know the frequency value the controller can perform a good control according to its initial system values. To do this, it is multiplied by the minimum frequency difference assigned to it, in this case 0.1 Hz, having the relationship Eq. (11).

$$\begin{aligned} F_{maxima a controlar} &= F_{inicial} + (K_p * 0.1 \text{ Hz}) \\ &= 60.12 + 28.8 * 0.1 = 63 \text{ Hz} \end{aligned} \quad (11)$$

This indicates that power equal to 0 can only be performed up to 63 Hz. Therefore, the controller must assign a variable called minimum change frequency, whose value is recommended to be less than or equal to 0.1 Hz, that said, it is described by Eq. (12).

$$F_{mc} \leq 0.1 \text{ Hz} \quad (12)$$

4. REACTIVE POWER

For reactive power, the ranges defined in Figure 7 align with the regulatory framework. Based on Figure 7, Table 2 is constructed.

Similar to active power, the control ramp for reactive power is determined by a percentage, as illustrated in Figure 7. This figure demonstrates that adjustments can be either negative or positive to achieve target values above or below those provided at the time of disturbance, depending on the requirements of each control mode. For power control, two scenarios are established: one in OL and the other in CL. Explanations for each scenario are provided below.

4.1 Open loop reactive power control

For open-loop reactive power control, a power value (QCONSIGNA) is considered to be the final objective. The grid operator and the solar park operator can manage this. The block diagram of the control in this mode of operation is shown in Figure 7.

Table 2. Ranges of reactive power in relation to active power

Q/Pn (pu)	P/Pn (pu)
$-0.33 = \frac{Q}{Pn}$	$0.2 < P/Pn < 0.95$
$-0.33 < \frac{Q}{Pn} < 0.288$	$25/51 * (\frac{Q}{Pn}) + 189/170$ Only if $0.95 \leq \frac{P}{Pn} \leq 1$
$-0.33 < \frac{Q}{Pn} < -0.1$	$-10/23 * (\frac{Q}{Pn}) + 13/230$ Only if $0.1 \leq \frac{P}{Pn} \leq 0.2$
$-0.10 \leq \frac{Q}{Pn} \leq 0.10$	0.1 only yes $P/Pn = 0.1$
$-0.228 \leq \frac{Q}{Pn} \leq 0.228$	1 only yes $P/Pn = 1$
$0.1 < \frac{Q}{Pn} < 0.33$	$10/23 * (\frac{Q}{Pn}) + 13/230$ Only if $0.1 \leq \frac{P}{Pn} \leq 0.2$
$0.288 < \frac{Q}{Pn} < 0.33$	$-25/51 * (\frac{Q}{Pn}) + 189/170$ Only if $0.95 \leq \frac{P}{Pn} \leq 1$
$0.33 = \frac{Q}{Pn}$	$0.2 < P/Pn < 0.95$

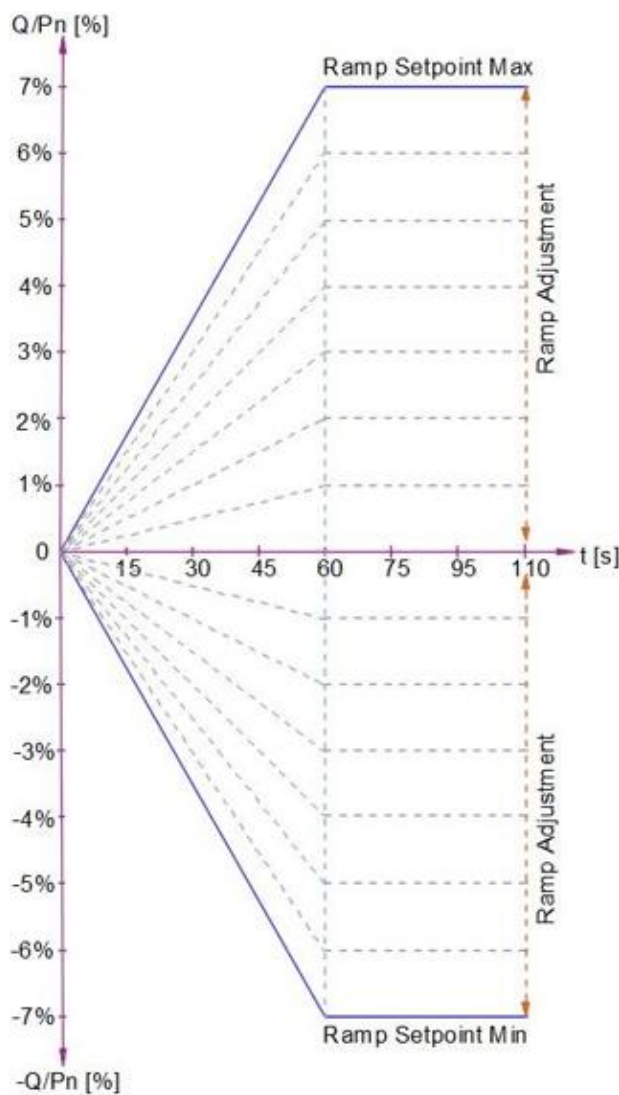


Figure 7. Graph of ramp control reactive power

The QSETPONT will be the target reactive power, which will pass through the ramp control and vary its behavior from the ramp setpoint assigned to it, varying between 0.1% and 7%; this last percentage will be the maximum ramp value that is suggested to be given [9].

The ramp control will take the necessary steps to reach the target value, providing QTOT output as the total ratio of reactive power to be reached at the connection point. Each group of panels in the solar park is represented by a set of "Smart data loggers," which allows each group of solar panels to be recorded and monitored and thus obtain the behavior of the inverters. They are assigned a value of "K" that will be a percentage constant that each SDL will be able to supply according to its associated installed capacity.

The QSDL block diagram shows a different group of "Smart data loggers", represented by Eq. (13):

$$Q_{TOT} = Q_{SDL1} + Q_{SDL2} + Q_{SDL3} + \dots + Q_{SDLn} \quad (13)$$

Considering that each QSDL is equivalent to those described by Eq. (14):

$$\begin{aligned} Q_{SDL1} &= K_1 * Q_{TOT}; Q_{SDL2} = K_2 * Q_{TOT}; \\ Q_{SDL3} &= K_3 * Q_{TOT}; Q_{SDLn} = K_n * Q_{TOT} \end{aligned} \quad (14)$$

The sum of each QSDL must be equal to QTOT, so it can be concluded that the sum of all the "K" must be equal to "1", considering values per unit, we arrive at Eq. (15).

$$K_{TOTAL} = K_1 + K_2 + K_3 + \dots + K_n = 1pu \quad (15)$$

The output of the QSDL represents the inverters associated with each set of panels in the photovoltaic park, which will ultimately make the power directive as requested and use the existing capacity in each set.

According to the power ranges described in Table 2. Ranges of reactive power in relation to the active power, the QCONSIGNA is defined, which is directly related to the photovoltaic park's active power.

The behavior at the coupling point depends on the type of reactive power to be compensated, negative or positive; in both cases, it is described by Eq. (16).

$$Q_{TOT} = \begin{cases} \frac{Q_{TOT}}{Q_{SDL1} + Q_{SDL2} + Q_{SDL3} + \dots + Q_{SDLn}} = 1pu \text{ Si } Q_{consigna} \geq 0 \\ \frac{-Q_{TOT}}{Q_{SDL1} + Q_{SDL2} + Q_{SDL3} + \dots + Q_{SDLn}} = -1pu \text{ Si } Q_{consigna} < 0 \end{cases} \quad (16)$$

4.2 Closed-loop reactive power control

The operation of closed-loop control is similar to open-loop control, but the output of the so-called ramp control must be fed back and compared to the power delivered by the meter at the connection point; therefore, it becomes the setpoint of the PI closed-loop controller.

Considering the abovementioned approach, a block diagram is designed for this control mode, as seen in Figure 8.

The acting signal delivered by the equipment at the connection point must be proportional to the difference between the input and output power to decrease the error and make it as close to zero as possible, as shown in Eq. (17).

$$Error = Q_{SP} - Q_{PC} \quad (17)$$

For this case, parameters for the controller must be defined, such as gain (P) and integral time (I).

Gain (P): This will be a minimum reactive power that we want to keep within a permissible margin of error.

Integral Time (I): This is the time it takes for each assigned

power gain scale to start a new scale.

The goal of the PI is to reach the desired value, in this case

the margin of error with a gain and integration time that the operator assigns.

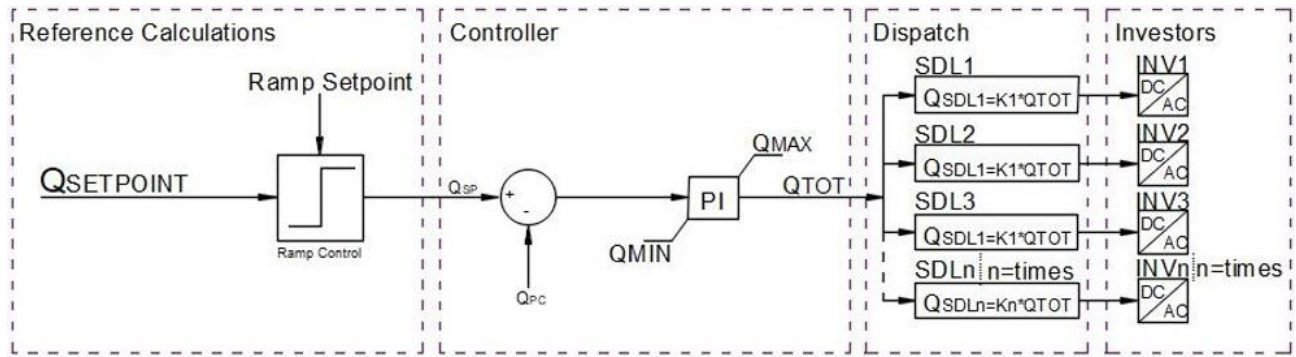


Figure 8. Block diagram closed loop reactive power control mode

4.3 Voltage control based on reactive power

In controlling voltage from the reactive power, new feedback must be considered that will depend on the voltage variations at the connection point [10], the maximum capacity that the plants can supply according to their declared power, and the limits established in CREG 060 of 2019. Considering the definition of voltage statism made in Annex 1 of CNO 1532, where the voltage control operation of photovoltaic solar plants is verified, where the voltage statism is determined according to the reactive power variation for each unit of percentage voltage variation and is expressed in Eq. (18).

$$Rv = \frac{\Delta U / U_{nom}}{\Delta Q / P_{nom}} \times 100\% \quad (18)$$

where,

ΔU : Magnitude of voltage variation.

ΔU : $U_{final} - U_{initial}$.

U_{nom} : Nominal voltage at the connection point.

ΔQ : Magnitude of variation in reactive power due to frequency variation.

ΔQ : $Q_{final} - Q_{initial}$.

P_{nom} : Nominal power of the park.

As established in the standard, the following parameters will be taken into account:

Dead Band: $0.98pu \leq V_{nom} \leq 1.02 pu$.

Statism: R must be assigned from the start. (9% – 15.5%).

$Q_{initial}$: Varies according to what is available in the park at the time of the disturbance.

Q_{final} : Voltage disturbance at the coupling point.

Undervoltage: $V_{nom} < V_{nom} - 0.2$.

Overtoltage: $V_{nom} > V_{nom} + 0.2$.

Once these parameters have been defined, a voltage control can be carried out concerning the statism ranges established in the standard and the normal operating ranges of the voltage at the coupling point. Table 3 presents the characteristics of these operating ranges.

Table 3. Voltage ranges

V (pu)	Rank	Control
$V < 0.9$		Minimum voltage limit of park operation. Protections must act.
$0.9 \leq V < 0.95$	Undervoltage	The wind farm will deliver maximum reactive power capacity.
$0.95 \leq V < 0.98$		The plant must deliver defined reactive power in a 20-second restoration time until it reaches a value equal to or greater than 0.98.
0.98		
1	Deadband	The control system does not operate in this voltage range, the wind farm must operate normally.
1.02		
$1.02 < V \leq 1.05$		The plant must deliver defined reactive power in a 20-second restoration time until it reaches a value equal to or less than 1.02.
$1.05 < V \leq 1.10$	Overvoltage	The wind farm will deliver the minimum reactive power capacity.
$V < 1.10$		Minimum voltage limit of park operation. Protections must act.

In Colombia, the frequency, voltage, and P_n/Q ranges are based on CREG resolution 229 of 2021 and the IEEE Standard for Interconnection and Interoperability of Distributed Energy Resources with Associated Electric Power Systems Interfaces. Considering the ranges of Table 3, the statism of 15.5%, and the minimum statism corresponding to ideal behavior, Figure 9 shows the voltage control.

In Figure 9, it can be seen that the slope of the ramp varies according to the statism setpoint; therefore, the higher the statism value, the lower the slope of the ramp, but its response time will be slower, in CNO 1531, it provides a reference value

of 15.5%; therefore, it is taken as the maximum value of statism within the adjustment made.

To evaluate the ideal statism, the percentage of statism that must guarantee the minimum or maximum reactive power capacity when changes due to Undervoltage or overvoltage occur is determined, see Eq. (19).

$$Q_{MAX} = 0.33 Q/P_n \text{ and } Q_{MIN} = -0.33 Q/P_n \quad (19)$$

In view of the above, Eq. (18) is used, and the values corresponding to the undervoltage disturbances will be taken,

these values are:

$U_{initial}$: 0.98 pu ($U_{nom} - Bmuerta$) is where the Undervoltage control will start.

U_{final} : 0.95 pu (Undervoltage value where Qmax should be supplied).

U_{nom} : 1 pu (Nominal System Voltage).

Q_{final} : 0.33 pu (Maximum reactive power to be supplied).

$Q_{initial}$: 0 pu (Ideal behavior of the system before the disturbance).

P_{nom} : Nominal power of the park.

Based on equation Eq. (18), the way in which it can be rewritten, see Eq. (20).

$$Rv = \frac{(U_{final} - U_{initial}) / U_{nom}}{(Q_{final} - Q_{initial}) / P_{nom}} \times 100\% \quad (20)$$

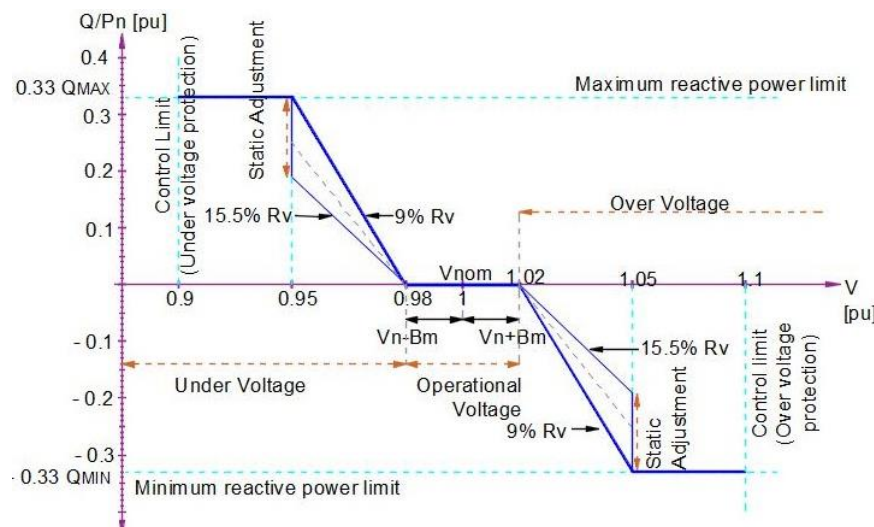


Figure 9. Tension control graph according to statism setting

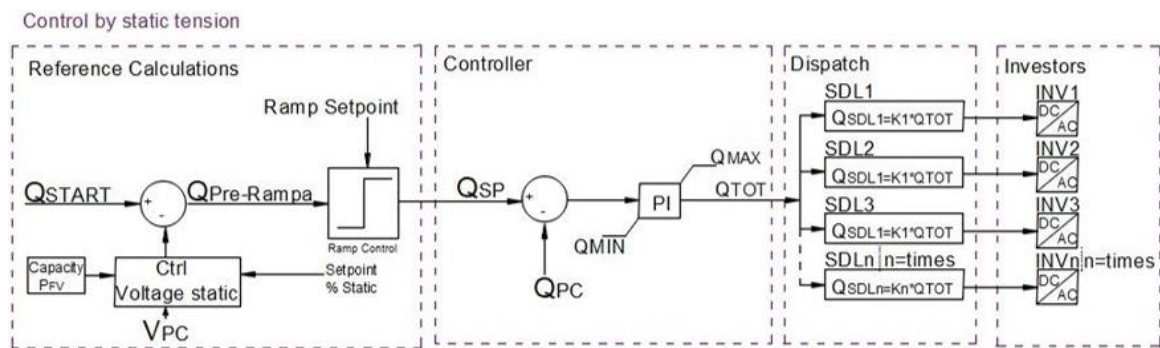


Figure 10. Block diagram of voltage control mode

Finally, the input is the voltage that is at the connection point and the one that must validate the behavior in which it is located.

To carry out the voltage control, the voltage changes at the connection point are considered; we use Eq. (18), which will be cleared in Eq. (21).

$$Q_{final} = Q_{initial} \pm \frac{(V_{final} - V_{initial}) * P_{nom}}{Rv * V_{nom}} \quad (21)$$

The values are replaced and the ideal statism percentage is calculated.

This value is applicable for Undervoltage and overvoltage because, in both cases, the straight slope has the same behavior since the result of the reactive power voltage deltas is the same.

Additionally, the relationship of the actual power capacity of the photovoltaic park must also be known to obtain the ability of the reactive power that can be supplied; this variable can be determined from the approach made in the Table 2.

The behavior of voltage control due to statism is presented in Figure 10.

In this control mode, new feedback will depend on the voltage statism controller; this new block will have the statism that the operator assigns as inputs and must be within an established range. The information will allow us to know the actual power capacity of the park to develop the content of reactive power that must be supplied.

where,

Q_{final} : New value of reactive power to be supplied or absorbed.

$Q_{initial}$: The reactive power at which the photovoltaic park is located before the voltage disturbance.

P_{nom} : Declared nominal power of the photovoltaic park.

V_{final} : Voltage disturbance to be corrected.

$V_{initial}$: Voltage before the disturbance the system was working on.

V_{nom} : Nominal system voltage.

Rv : Percentage of statism assigned in the voltage control.

5. METEOROLOGICAL VARIABLES FOR PHOTOVOLTAIC SOLAR PLANTS CONNECTED TO THE STN AND STR

Article 23 of Resolution 060 of 2019 of the Energy and Gas Regulatory Commission (CREG) specifies the protocols for quality verification, reliability of measurement and reporting to the CND of the meteorological variables corresponding to global horizontal irradiance (*GHI*), in-plane irradiance (*POA*), posterior temperature of the photovoltaic panel (*T_{mod}*) and ambient temperature (*T_{amb}*) for photovoltaic solar plants [11, 12].

The meteorological variables that must be measured and reported to the CND by the operating agents of photovoltaic solar plants are:

- *Irradiance [G]*: Incident radiant power flux per unit area.
- *In-plane irradiance [or] G_iPOA*: The sum of the direct, diffuse, ground-reflected incident irradiance on an inclined

surface parallel to the plane of the photovoltaic cell.

• *Modules*. It is also known as *POA plane of array irradiance*.

• *Global horizontal irradiance ()*: Direct irradiance *GHI* plus diffuse irradiance impinging on a horizontal surface.

• *Ambient temperature ()*: *T_{amb}* This is the temperature of the atmosphere in the vicinity of the solar photovoltaic plant location [°C].

• *Module temperature ()*: *T_{mod}* Operating temperature of photovoltaic cells [°C].

The IEC 61724-1 standard [13] defines the classification of the Requirements of the monitoring system of solar plants connected to interconnected systems and specifies that these must be class A (high accuracy); this classification is shown in Table 4. Once the application of the system has been determined, the requirements for the control of the irradiance variables and the temperature variables defined in Article 23 of the CREG are listed in Table 5.

Table 4. Classification of monitoring systems for solar photovoltaic plants

Application of the Monitoring System	Class A	Class B	Class C
Evaluation of basic system performance	YES	YES	YES
Performance assurance documentation	YES	YES	NO
System loss analysis	YES	YES	NO
Evaluation of the interaction with the power grid	YES	NO	NO
Fault Location	YES	NO	NO
Photovoltaic technology assessment	YES	NO	NO
Measure of PSF degradation	YES	NO	NO

Table 5. Requirements for the control of irradiance variables and temperature variables

Parameter	Symbol	Unit	Purpose	Parameter Control
In-plane irradiance (POA)	Gi	$\frac{W}{m^2}$	Radiation/Solar Resource	The control is carried out using sensors placed in the modules' plane and appropriately distributed in the solar plant area. Mounting: The sensor's aperture should have a 160° field, inclined at the same angle as the solar cell panels. Installation: It must be done on the panels' supports or on an extension made to these supports. Measurement sensor: Reference photovoltaic devices measure the useful solar irradiance that affects the power output of the photovoltaic solar plant. Uncertainty: Number of Sensors: Main & Backup Sampling Interval: 10s
Global horizontal irradiance	GHI	$\frac{W}{m^2}$	Solar resource, connection with historical and satellite data	Control uses sensors (main and back-up) oriented horizontally. Mounting: Representative Location Installation: They must be mounted horizontally, with no incident shadows Measurement sensor: A horizontally oriented irradiance sensor is used, especially thermopile pyranometers (useful irradiance variation from 1% to 3%). Uncertainty: $\leq 3\%$ Range: 0 W/m ² – 1500W/m ² Resolution: 1000 W/m ² and 1500 W/m ² . Number of sensors: <i>see table 8. Minimum number of in-plane irradiance (POA) and temperature sensors of photovoltaic modules (T_{amb}) according to the capacity of the solar photovoltaic (AC) plant.</i> Sampling Interval: 10s
Photovoltaic module temperature	T _{mod}	°C	Temperature-related losses are determined	Positioning: (Plant – Properly distributed2 by the modules of the solar plant). (Module: Below the center of a cell at or near the center of the module) Permanent fixation: Polyester tape and epoxy adhesive Temporary fixation: Polyester tape Type: Type T or E Thermocouples, Resistance, Thermistors Geometry: Planes Resolution and uncertainty: $\leq 0.1^\circ\text{C}$ and $\pm 2^\circ\text{C}$ Sampling Interval: 10s
Ambient air temperature	T _{amb}	°C	Connection to historical data and temperature estimation of photovoltaic cells	Positioning: At a point far away from the solar panels and other plant installations, where the air circulates freely. Type: Conventional Resolution and uncertainty: $\leq 0.1^\circ\text{C}$ and $\pm 1^\circ\text{C}$ Sampling Interval: 1m

Table 6. Minimum number of in-plane irradiance (POA) and temperature sensors of photovoltaic modules (T_{amb}) according to the capacity of the solar photovoltaic (AC) plant

AC System Capacity	Number of Sensors
< 40 MW	2
≥ 40 MW and < 100 MW	3
≥ 100 MW and < 200 MW	4
≥ 200 MW and < 300 MW	5
≥ 300 MW and < 500 MW	6
≥ 500 MW and < 750 MW	7
≥ 750 MW	8

According to the system, it is essential to define the protocols to ensure reliability and quality when measuring in-plane irradiance, horizontal global irradiance, temperature of

photovoltaic modules, and ambient temperature in solar photovoltaic plants connected to the National Interconnected System (SIN).

The control and reporting of these variables are carried out in stages, implementing a class A monitoring system as described above [14].

The first stage corresponds to the proper selection of sensors, which will depend on the capacity of the photovoltaic plant as indicated in Table 6. The second to the requirements for their installation, and the third to the number and distribution of them.

First stage: The international regulation of the sensors must be taken into account when selecting them, as shown in Table 7.

Table 7. Selection of sensors according to their characteristics according to regulations

Variable	Instrument	Instrument Features
POA	Thermopile pyranometer	IDEAM uses IDEAM, CM11 and CMP6. For their operation, they can go parallel, horizontally, inclined and even the other way around. Response time: >15 seconds; 18 seconds Approximate instability: 0.5% Light beam: $\pm 1 \text{ W/m}^2$ Spectral sensitivity: ~2%; 4% Spectral band: varies between 305-2800nm and 335-2200nm; 280 to 2-2800 nm Sensitivity: 4 and 6; 5 and 20 $\frac{\mu\text{V}}{\text{W/m}^2}$
GHI	Reference Cell	The selection must be made taking into account the normal Select according to IEC 60904-2
T_{mod}	Type T or E Thermocouples Resistance Thermometers Thermistors	IDEAM uses IDEAM CMP6. For their operation, they can go parallel, horizontally, inclined and even the other way around. Response time: > seconds; 18 seconds Approximate instability: 0.5% Light beam: $\pm 10 \text{ W/m}^2$ Spectral sensitivity: ~2%; 4% Spectral band: varies between 305-2800 nm and 335-2200 nm; 280 to 2-2800nm Sensitivity: 4 and 6; 5 and 20 $\frac{\mu\text{V}}{\text{W/m}^2}$
T_{amb}	Conventional	The selection must be made taking into account the Select according to IEC60904-2 standard Plans Resistance with efficient low temperature per $^{\circ}\text{C} \leq 10\text{ppm}$ Conventional

Second stage: The requirements for installing the irradiance and temperature sensors are described in Table 8.

Irradiance sensors should be located in places with no incident shadows, other than those of the atmosphere.

Table 8. Requirements for the installation of irradiance sensors

POA	They must be properly distributed in the solar plant, without incident shadows. The assembly must be carried out on the supports of the panels or an extension made to these supports.
GHI	They should be mounted horizontally, with no incident shadows.

The data in Table 9 must be considered for the installation of temperature sensors.

Third stage: The location of the temperature sensors in the modules must be as close as possible to the sensor installation points for the measurement of irradiance in the plane, this distribution must ensure that there are no incidences of disturbances unrelated to the monitored variables. Each agent

and the CND will agree on the number of in-plane irradiance (POA) and temperature data on the modules that will be transmitted to characterize the photovoltaic solar plant [15-20].

Table 9. Requirements for the installation of temperature sensors

Positioning	On the Floor (Proper Layout) In the module (permanent fixation and temporary fixation)
Guy	Type T or E thermocouples, Resistance thermometers, Thermistors
Geometry	It is recommended that they be flat
Resolution and Uncertainty	$\leq 0.1^{\circ}\text{C}$ and $\pm 2^{\circ}\text{C}$

The adequate distribution and quantity of sensors in the solar plant area for the measurement of these two variables: irradiance in the POA plane and the temperature in the T_{mod} modules, are those represented in Table 6; this ensures that the values of the meteorological variables are representative and that their value is not affected by anomalies such as light

reflections, shadows, different configurations of the solar module supports, therefore, it is essential that the entire extension of the plant by adjusting a representative radius according to the topography of each plant and the number of sensors, which is why it is recommended that the measurement points where the temperature sensors are going to be installed in the modules are the same ones where irradiance sensors are installed in the plane.

6. FREQUENCY CONTROL BEHAVIOR

This session describes the expected behavior from a 15 MW photovoltaic solar park regarding frequency control mode. The

aim is to demonstrate how such a generation system can be a backup to grid operators.

A static response of 6% will be assumed, throughout this discussion replacing values in Eq. (8). Additionally, we will consider a generation of 5 MW at the time of disturbance, categorizing behavior into three zones that cover scenarios likely at the grid connection point.

The following table depicts the behavior of a 15 MW capacity generation park under these conditions.

Ideal conditions at the connection point:

Maximum Active Power of PV: 15 MW

Static Response: 6%

Nominal Frequency: 60 Hz

Table 10. Typical compensation of the frequency control system

Frequency at PC (Hz)	Generation at Disturbance Moment PV (MW)	Final Power at PC (MW)	Power to be Supplied by the System (MW)	Compensation Ramp (%)	Final Frequency (Hz)	Zone
58	5	13.33	8.33	56%	60	Underfrequency
60	5	5.00	0.00	0%	60	Ideal Behavior
61	5	0.83	-4.17	-7%	60	Overfrequency

As shown in the Table 10, under frequency conditions at the grid connection point, the park must supply an additional 8.33 MW of active power, totaling 13.33 MW, below its maximum capacity of 15 MW.

Under ideal conditions, the system does not need to supply additional active power to maintain grid stability.

In the case of over frequency at the connection point, the park needs to absorb 4.17 MW, reducing its generation to 0.83 MW.

The foregoing demonstrates that the equations governing different control modes align with expected behaviors. It underscores their viability for use in photovoltaic solar parks, which generate electrical energy and function as backup systems for various interconnected electrical grids, thus meeting regulatory requirements.

7. CONCLUSIONS

To arrive at the frequency and voltage control modes related to statism, different analyses must be carried out regarding their behavior regarding the technical capacity of the photovoltaic park since this control mode is not viable when the plant's power is at its minimum generation values.

Inverters capable of generating capacitive and/or inductive reagents must be available for the reactive power control mode since the generation type in solar parks does not have this behavior.

The behavior of the frequency controller will depend on the statism assigned between the ranges established in the standard; this behavior will tend to be fast or slow in its response time; the lower the percentage of assigned statism, the faster its behavior will be, but in turn, the control range will be lower. Otherwise, if the rate of statism is higher, it will have a slower response time but a greater control range due to the graph's characteristics with respect to its slope.

For all the control modes exposed in this document, ramp control is significant since it will determine the time it will take to reach the desired value; this will have a response time that will depend on a ramp setpoint value that must be within what is established by the Colombian standard.

The control system cannot replace the functions of the protective equipment, so this equipment must have a coordination study according to the characteristics required in the regulatory framework.

It is essential to define the protocols for verifying reliability and quality when measuring global horizontal irradiance (*GHI*), in-plane irradiance (*POA*), posterior temperature of the photovoltaic panel (*T_{mod}*) and ambient temperature (*T_{amb}*) according to resolution 060 of 2019 of the CREG, these meteorological variables applicable to photovoltaic solar plants connected to the STN and STR must be directly related to the quality and quantity of energy generated necessary for the plant, therefore, the calculation of the number of sensors needed, their installation and positioning will allow adequate control to report to the CND.

ACKNOWLEDGMENTS

The authors thank the Oficina de Investigaciones of the Universidad Distrital Francisco Jose de Caldas for supporting this project.

REFERENCES

- [1] Simionescu, M., Radulescu, M., Belascu, L. (2024). The impact of renewable energy consumption and energy poverty on pollution in Central and Eastern European countries. *Renewable Energy*, 121397. <https://doi.org/10.1016/j.renene.2024.121397>
- [2] Guerra Sánchez, M., Assaf Montaño, J.C., Ascanio Mantilla, N.J. (2021). Implementación de energías renovables como garantía al derecho fundamental a un ambiente sano en Colombia. *Revista CES Derecho*, 12(2): 87-106. <https://doi.org/10.21615/cesder.6163>
- [3] Wang, H., Mao, L., Zhang, H., Wu, Q. (2024). Multi-prediction of electric load and photovoltaic solar power in grid-connected photovoltaic system using state transition method. *Applied Energy*, 353: 122138. <https://doi.org/10.1016/j.apenergy.2023.122138>

- [4] Guerrero, R.J.A., Pineda, A.S.R. (2022). Control de factor de potencia en una red fotovoltaica en la Parroquia Vuelta Larga, Esmeraldas–Ecuador. *Revista Social Fronteriza*, 2(2): 22-35. <https://doi.org/10.5281/zenodo.6429664>
- [5] González-Moreno, A., Marcos, J., de la Parra, I., Marroyo, L. (2023). Control method to coordinate inverters and batteries for power ramp-rate control in large PV plants: Minimizing energy losses and battery charging stress. *Journal of Energy Storage*, 72: 108621. <https://doi.org/10.1016/j.est.2023.108621>
- [6] Khelil, C.K.M., Amrouche, B., soufiane Benyoucef, A., Kara, K., Chouder, A. (2020). New Intelligent Fault Diagnosis (IFD) approach for grid-connected photovoltaic systems. *Energy*, 211: 118591. <https://doi.org/10.1016/j.energy.2020.118591>
- [7] Ye, B., Fu, Y., Zhang, S., Wang, H., Fang, G., Zha, W., Dwivedi, A.K. (2023). Closed-loop active control of the magnetic capsule endoscope with a robotic arm based on image navigation. *Journal of Magnetism and Magnetic Materials*, 565: 170268. <https://doi.org/10.1016/j.jmmm.2022.170268>
- [8] Messasma, C., Barakat, A., eddine Chouaba, S., Sari, B. (2023). PV system frequency regulation employing a new power reserve control approach and a hybrid inertial response. *Electric Power Systems Research*, 223: 109556. <https://doi.org/10.1016/j.epsr.2023.109556>
- [9] National Council for the Operation of the Electricity Sector (CNO). (2022). Agreement 1531 approving the technical requirements for voltage control for wind and solar photovoltaic plants connected to the SDL with net effective capacity or maximum declared power equal to or greater than 5 MW. <https://www.cno.org.co/content/acuerdo-1531-por-el-cual-se-aprueban-los-requisitos-tecnicos-para-el-control-de-tension>.
- [10] Zuo, H., Xiao, W., Ma, S., Teng, Y., Chen, Z. (2024). Reactive power optimization control for multi-energy system considering source-load uncertainty. *Electric Power Systems Research*, 228: 110044. <https://doi.org/10.1016/j.epsr.2023.110044>
- [11] AlSkaif, T., Dev, S., Visser, L., Hossari, M., van Sark, W. (2020). A systematic analysis of meteorological variables for PV output power estimation. *Renewable Energy*, 153: 12-22. <https://doi.org/10.1016/j.renene.2020.01.150>
- [12] Alberti, E L., Paludo, R., Portella, K.F., Bragança, M.D.O.G.P., Rocha, G.P.U., Mazur, M.M., Portella, A.C.F. (2023). New concept on 100.74 kWp floating solar photovoltaic plant and a real mechanical failures assessment: Case of study at Santa Clara hydroelectric power plant reservoir in southern Brazil. *Sustainable Energy Technologies and Assessments*, 60: 103455. <https://doi.org/10.1016/j.seta.2023.103455>
- [13] Muñoz-Rodríguez, F.J., Snytko, A., de la Casa Hernández, J., Rus-Casas, C., Jiménez-Castillo, G. (2023). Rooftop photovoltaic systems. New parameters for the performance analysis from monitored data based on IEC 61724. *Energy and Buildings*, 295: 113280. <https://doi.org/10.1016/j.enbuild.2023.113280>
- [14] Ma, M., He, B., Wang, N., Shen, R. (2022). A method for monitoring the solar resources of high-scale photovoltaic power plants based on wireless sensor networks. *Sustainable Energy Technologies and Assessments*, 53: 102678. <https://doi.org/10.1016/j.seta.2022.102678>
- [15] Sun, Y., Zhu, D., Li, Y., Wang, R., Ma, R. (2023). Spatial modelling the location choice of large-scale solar photovoltaic power plants: Application of interpretable machine learning techniques and the national inventory. *Energy Conversion and Management*, 289: 117198. <https://doi.org/10.1016/j.enconman.2023.117198>
- [16] Mainil, R.I., Afif, F., Arief, D.S., Mainil, A.K., Aziz, A. (2024). Performance comparison of photovoltaic (PV), heat pipe photovoltaic/thermal (HP-PV/T), and heat pipe solar thermal collectors (HP-STC): Energy analysis. *International Journal of Heat and Technology*, 42(3): 897-904. <https://doi.org/10.18280/ijht.420318>
- [17] Moulay, F., Habbati, A., Lousdad, A. (2022). The design and simulation of a photovoltaic system connected to the grid using a boost converter. *Journal Européen des Systèmes Automatisés*, 55(3): 367-375. <https://doi.org/10.18280/jesa.550309>
- [18] Wibowo, S., Arifin, Z., Rachmanto, R.A., Himawanto, D.A., Prasetyo, S.D. (2024). Optimization of photovoltaic performance using a water spray cooling system with different nozzle types. *International Journal of Computational Methods and Experimental Measurements*, 12(1): 9-19. <https://doi.org/10.18280/ijcmem.120102>
- [19] Abdullah, A.R., Majel, B.M. (2022). Numerical study of photovoltaic panel thermal efficiency using multi-cooling process. *International Journal of Heat and Technology*, 40(4): 1100-1106. <https://doi.org/10.18280/ijht.400429>
- [20] Prasetyo, S.D., Arifin, Z., Prabowo, A.R., Budiana, E.P., Mohd Rosli, M.A., Alfaiz, N.F., Bangun, W.B. (2023). Optimization of photovoltaic thermal collectors using fins: A review of strategies for enhanced solar energy harvesting. *Mathematical Modelling of Engineering Problems*, 10(4): 1235-1248. <https://doi.org/10.18280/mmep.100416>